

Zeynel Demirel
Cüneyt Güler

Hydrogeochemical evolution of groundwater in a Mediterranean coastal aquifer, Mersin-Erdemli basin (Turkey)

Received: 25 July 2005
Accepted: 16 September 2005
Published online: 11 November 2005
© Springer-Verlag 2005

Z. Demirel · C. Güler (✉)
Department of Geological Engineering,
Engineering Faculty, Mersin University,
33343 Mersin, Turkey
E-mail: cguler@mersin.edu.tr
Tel.: +90-324-3610001
Fax: +90-324-3610032

Abstract In this study, hydrogeologic and hydrochemical information from the Mersin-Erdemli groundwater system were integrated and used to determine the main factors and mechanisms controlling the chemistry of groundwaters in the area and anthropogenic factors presently affecting them. The PHREEQC geochemical modeling demonstrated that relatively few phases are required to derive water chemistry in the area. In a broad sense, the reactions responsible for the hydrochemical evolution in the area fall into four categories: (1)

silicate weathering reactions; (2) dissolution of salts; (3) precipitation of calcite, amorphous silica and kaolinite; (4) ion exchange. As determined by multivariate statistical analysis, anthropogenic factors show seasonality in the area where most contaminated waters related to fertilizer and fungicide applications that occur during early summer season.

Keywords Coastal aquifer · Water–rock interaction · Principal components analysis · Cluster analysis · Mersin

Introduction

The development of groundwater resources for water supply is a widespread practice in the Mediterranean coastal region of Turkey, favored by the existence of basins with thick Quaternary deposits that form aquifers with good-quality water (Demirel 2004). The Mersin-Erdemli basin (MEB) is particularly productive (Fig. 1). The Mediterranean coastline stretching from the city of Mersin to the Erdemli region is heavily populated with recent (last 15 years) urban developments (e.g., villas, apartment complexes, and multi-storey buildings), which are mostly occupied during summer season for vacation purposes. Due to an increased population influx from the surrounding cities, especially during the peak season (May to September); the population of this region increases several folds (e.g., 2–4 times). The MEB is not only an urban area but it is also surrounded by densely cultivated orchards (mostly citrus), traditional vegetable farms and greenhouse cultivations, where farming activities continue all year long due to favorable climate.

In the MEB area, urban and agricultural expansions have caused an ever-growing need for fresh water. In this region, water supply for most municipalities, domestic use water for urban developments and irrigation water for agricultural activities is almost exclusively provided through hand dug or drilled wells. In addition to obvious primary uses of water for domestic use (e.g., washing and bathing) the quantities required have been greatly increased by secondary demand, principally for gardening, landscaping, and water for swimming pools of the villas, apartment complexes, etc. These supplies are mostly required during the main holiday season, which coincides with the driest period. Therefore, water resources in the MEB area are subject to intensive demands, stresses and pollution risks (Demirel 2004) and similar problems were reported in the other Mediterranean countries (e.g., Pulido-Leboeuf 2004).

Population dynamics and agricultural activities in this region have important implications from the groundwater chemistry standpoint, especially in the near-shore area, for local communities who rely upon

coastal aquifers directly for their water supply. Despite its importance, little is known about the natural phenomena that govern the chemical composition of groundwater in this region or the anthropogenic factors that presently affect them. This study tries to answer mainly these questions. The main objectives of this paper are: (1) to assess the chemistry of groundwater and (2) to identify the anthropogenic factors that presently affect the water chemistry in the region by using multivariate statistical and geochemical modeling techniques.

Site description

The MEB is situated in the Mediterranean Sea region of the southeastern part of Turkey and extends from 36°30′–36°45′ of latitude north to 34°15′–37°30′ of longitude west (Fig. 1). The MEB area is bounded by the Taurus Mountains on the northern side and by the Mediterranean Sea on the southern side. The southern portion of the MEB area is a delta plain made up of sediments mainly from Alata River in the west and partly by Tece, Arpaç, and Mezitli creeks in the east direction. The flow regimes of these creeks are strongly dependent on the seasonal rains. These creeks flow only 3–4 months in a year and their average discharges are 2–3 m³/s. Topographic structure in the north of the investigated area (Taurus Mountains) is rugged with altitudes ranging from 300 to 1,100 m.

In the MEB area, climate is characterized by hot and dry periods in summer and by warm and wet periods in winter, which is typical for the coastal zones around the Mediterranean Sea. According to 30-year monthly averages, lowest mean temperature occurs in January (10°C) and highest mean temperature in August (28°C). The mean annual temperature in this area is 18.6°C. Showers start in October, and continue till mid April and the maximum rainfall occurs in December. The MEB area receives slightly higher than 500 mm of precipitation annually, and extended periods (i.e., 3–4 months) without precipitation are common. Monthly average atmospheric temperatures and precipitation for a 30-year period (1961–1991) at the Erdemli station are presented in Fig. 2.

Rocks and unconsolidated deposits in the area can be divided into three geologic units (Senol 1998): (1) upper Cretaceous mersin ophiolitic mélange; (2) Tertiary units; (3) Quaternary basin-fill deposits. A simplified stratigraphic column showing associations between all rocks and unconsolidated sediments is shown in Fig. 3. Mersin ophiolitic mélange (upper cretaceous) is generally found in the northern part of the study area within deep canyons and shows serpentinization (Fig. 1). Ophiolitic mélange contains various rocks with differing compositions including gabbro, harzburgite, verlite, dunite, clinopyroxenite, diabase, and radiolarite.

Ophiolitic mélange also contains substantial amounts of chromite mineralizations with chromite (Cr₂O₃) contents ranging between 52–60% (Yaman 1991).

Tertiary units are composed of oligo-miocene gildirli formation, lower-middle miocene karaisali formation and güvenç formation, middle-upper miocene kuzgun formation, and upper miocene-pliocene handere formation (Fig. 1). Tertiary rocks consist of a succession of marine, lacustrine, and fluvial deposits, which display transitional characteristics both vertically and areally in the study area (Senol 1998).

The Quaternary basin-fill deposits are a heterogeneous mixture of metamorphic, volcanic, and sedimentary rock detritus ranging from clay to boulder size. The mixture includes stream alluvium, stream-terrace deposits, fan deposits, delta deposits, shore deposits, caliche (calcrete), and Terra Rosa deposits (Mediterranean red soil) (Senol 1998). The basin-fill deposits vary greatly in lithology and grain-size, both vertically and areally. Accordingly, the hydraulic properties of these deposits can differ greatly over short distances, both laterally and vertically.

Materials and methods

Sample collection and analytical techniques

For chemical analysis, a total of 32 water samples from the MEB (from 6 springs, 11 wells, and 1 seawater sampling locations) were obtained during 2002 from two separate sampling campaigns (May and August) at the sampling points shown in Fig. 1. This period was chosen because it coincides with the maximum water abstraction from the MEB aquifer and minimum precipitation and recharge in the area. Table 1 summarizes the chemical analysis results for water samples collected from the MEB. One spring (sample no. 7) was sampled only once in August and two wells (samples 13 and 14) were sampled only once in August and May, respectively due to various reasons. Mediterranean Sea water was sampled only once in May. Therefore, there are only 14 locations that were sampled twice during both May and August 2002 sampling campaigns.

Water samples obtained from the wells are from various depths because the wells in the area vary greatly in depth. Average well depth is 15 m for hand dug wells and 87 m for drilled wells. Electrical conductivity (EC) and pH were monitored during pumping, and samples were collected only when values stabilized or after at least three well volumes had been purged. Water samples obtained from the springs were collected at the spring orifice. Measurements of EC and pH were made in the field using a pH/Cond 340i WTW meter. For the pH measurements the electrode was calibrated against pH buffers at each location. Two aliquots were taken from

Fig. 1 Map showing the water sampling locations and geology of the study area

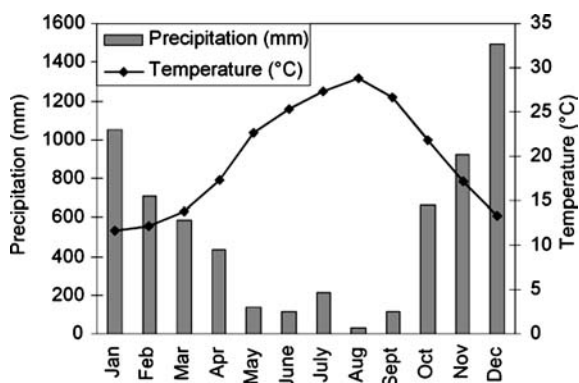
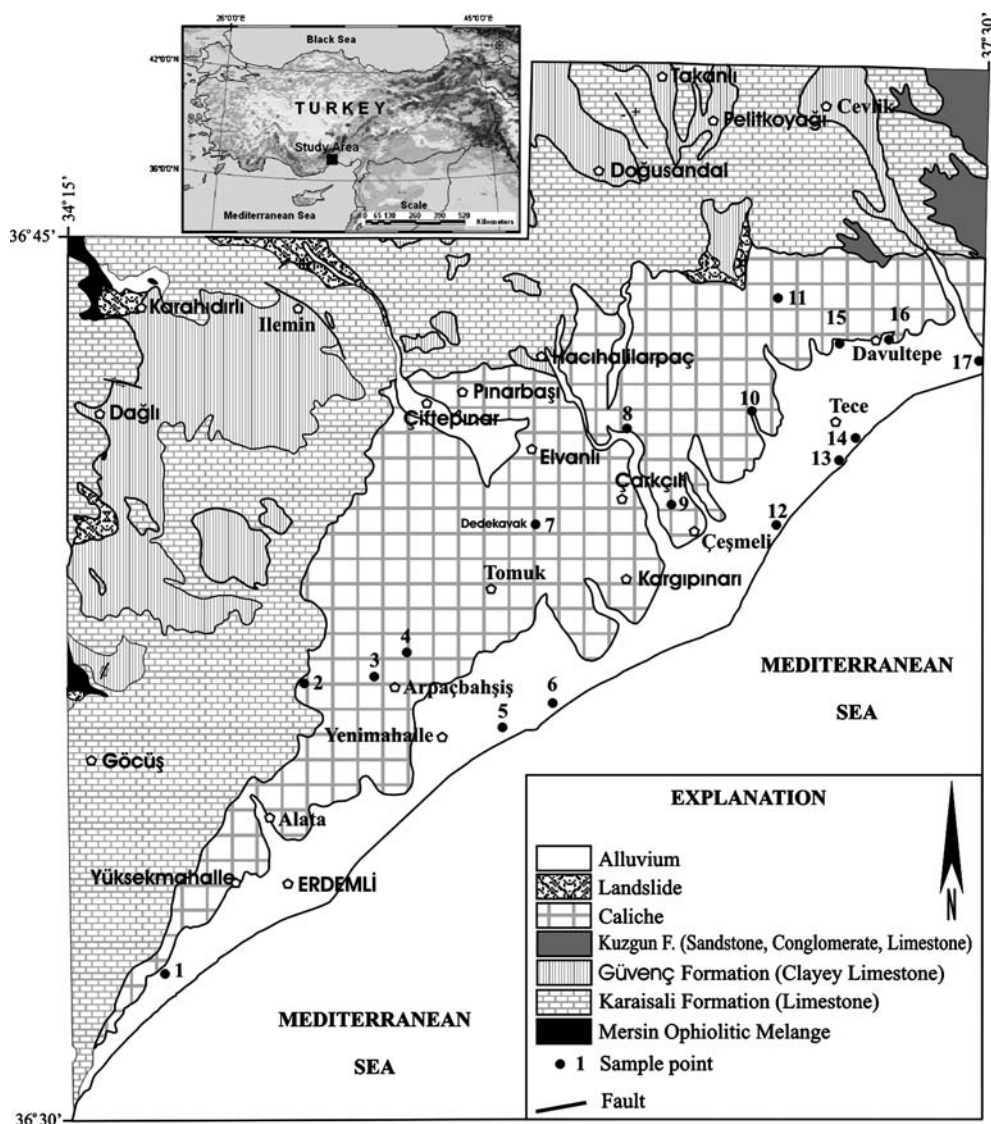


Fig. 2 Monthly average atmospheric temperatures (°C) and amount of precipitation (mm) for a 30-year period (1961–1991) at the Erdemli station

each sampling location; one for cation and the other for anion analysis. Aliquots were filtered through a 0.45-mm Millipore cellulose type membrane and stored in HDPE bottles. The sample bottles were rinsed three times with the filtered sample water before they were filled. Then, 0.25 ml/L of HNO₃ (nitric acid) was added to the first aliquot to prevent precipitation. The samples were refrigerated at 4°C until analysis. Cations were analyzed by inductively coupled plasma (ICP) and anions by ion chromatography (IC). SiO₂ was analyzed mainly by visible spectrophotometry. Bicarbonates were determined by titration in the laboratory. Samples were analyzed in the laboratory of General Directorate of Mineral Research and Exploration (MTA) of Turkey in Ankara. Each analysis was checked for accuracy by calculating their percent charge balance errors (%CBE)

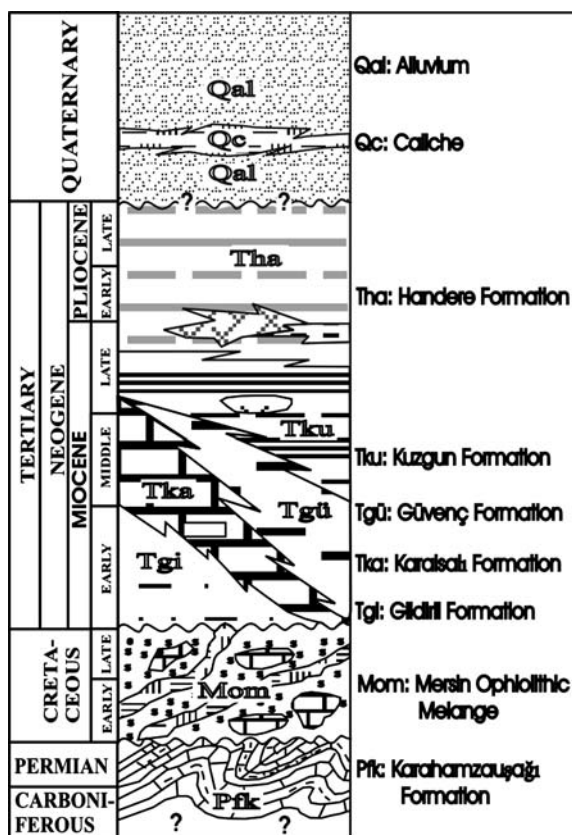


Fig. 3 A general stratigraphic section for the MEB area

(Table 1). No samples in the database have a CBE greater than $\pm 7\%$.

Statistical analysis

The Statistica[®] Release 5.5 (StatSoft Inc. 2000) commercial software package was utilized for the multivariate statistical analysis techniques performed. All 12 hydrochemical variables measured (consisting of EC, pH, Ca, Mg, Na, K, Cl, SO₄, HCO₃, F, SiO₂, and NO₃) were utilized in the statistical analyses. The water samples (samples 7, 13, 14, and 18), which are only sampled during one of the two sampling campaigns, were not included in the multivariate statistical analysis. For statistical analysis, all the variables were log-transformed and more closely correspond to normally distributed data. Subsequently, they are standardized to their standard scores (z -scores) as described by Güler et al. (2002). Standardization scales the data to a range of approximately -3 to $+3$ standard deviations (σ), centered about a mean (μ) of zero, giving each variable equal weight in the multivariate statistical analyses. Without scaling, the results are influenced most strongly by the variable with the greatest magnitude (Judd 1980).

The hierarchical cluster analysis (HCA) and principal components analysis (PCA) were used for the multivariate analyses. Advantages and uses of the HCA and PCA in hydrogeochemistry and the mathematical formulation behind these techniques are thoroughly discussed in Swanson et al. (2001) and in Güler et al. (2002). However, these techniques will be briefly described here.

Hierarchical cluster analysis (HCA)

Hierarchical cluster analysis is a powerful tool for analyzing water chemistry data (Reeve et al. 1996; Ochsenkühn et al. 1997) and has been used to formulate geochemical models (Meng and Maynard 2001). This method groups samples into distinct populations (a.k.a. clusters) that may be significant in the geologic/hydrologic context, as well as from a statistical point of view (Güler et al. 2002). The classification of samples according to their parameters is termed Q-mode classification. In this study, Q-mode HCA was used to classify the samples into distinct hydrochemical groups. The Ward's linkage method (Ward 1963) was used in this analysis. A classification scheme using Euclidean distance (straight line distance between two points in c -dimensional space defined by c variables) for similarity measurement, together with Ward's method for linkage, produces the most distinctive groups where each member within the group is more similar to its fellow members than to any member outside the group (Güler et al. 2002).

Principal components analysis (PCA)

As a multivariate data analytic technique, PCA reduces a large number of variables (measured physical parameters, major anions and cations in water samples) to a small number of variables which are the principal components (PCs) (Qian et al. 1994). More concisely, PCA combines two or more correlated variables into one variable. This approach has been used to extract related variables and infer the processes that control water chemistry (Helena et al. 2000; Hildago and Cruz-Sanjulian 2001).

Varimax rotation is applied to the PCs in order to find factors that can be more easily explained in terms of hydrochemical or anthropogenic processes (Helena et al. 2000). This rotation is called Varimax because the goal is to maximize the variance (variability) of the "new" variable, while minimizing the variance around the new variable (StatSoft Inc. 1997). The number of PCs extracted (to explain the underlying data structure) is defined by using the "Kaiser criterion" (Kaiser 1960) where only the PCs with eigenvalues greater than unity are retained. In other words, unless a PC extracts at least

Table 1 Chemistry of the water samples from two separate sampling campaigns (May and August 2002). Concentrations are in milligram per liter

ID	Sample source	Sample Date	EC ^a	pH	Ca	Mg	Na	K	Cl	SO ₄	HCO ₃	F	SiO ₂	NO ₃	% CBE ^b	Water Facies	Lithology ^d
1	Spring	05/2002	600	7.6	72.8	20.3	12.0	1.0	22.6	14.6	317	0.2	11.3	0.1	-2.48	Ca-Mg-HCO ₃	KF
		08/2002	623	7.2	75.2	19.2	11.0	1.0	31.8	10.8	331	0.2	14.8	8.0	-5.82	Ca-Mg-HCO ₃	KF
2	Spring	05/2002	492	7.9	51.6	20.9	8.0	1.0	16.1	12.4	263	-	10.0	10.0	-3.67	Ca-Mg-HCO ₃	KF
		08/2002	578	7.6	66.9	22.1	6.8	1.0	28.0	10.2	260	0.3	13.1	8.0	+1.84	Ca-Mg-HCO ₃	KF
3	Spring	05/2002	500	7.8	77.5	11.7	6.0	1.0	8.8	11.9	293	0.2	10.0	7.6	-1.85	Ca-HCO ₃	KF
		08/2002	546	7.5	60.3	12.3	5.9	2.3	14.2	8.6	260	0.1	10.0	5.1	-5.56	Ca-Mg-HCO ₃	KF
4	Spring	05/2002	774	7.4	65.0	42.4	34.0	4.4	34.7	43.6	419	0.5	28.5	12.9	-2.67	Mg-Ca-HCO ₃	KF
		08/2002	555	7.3	61.9	16.5	7.9	1.7	22.0	11.4	266	0.3	12.6	6.1	-3.98	Ca-Mg-HCO ₃	KF
5	Well	05/2002	750	7.7	63.2	49.9	14.0	1.3	26.3	54.2	383	-	29.5	26.4	-1.54	Mg-Ca-HCO ₃	A
		08/2002	730	7.9	48.1	47.9	15.6	1.3	38.0	38.2	343	0.7	31.0	17.9	-3.24	Mg-Ca-HCO ₃	A
6	Well	05/2002	645	7.5	54.7	32.9	11.0	1.7	21.4	39.6	311	0.3	18.4	13.6	-4.67	Ca-Mg-HCO ₃	A
		08/2002	685	7.4	61.0	37.6	9.4	1.3	32.0	31.6	326	0.4	22.7	17.3	-2.56	Mg-Ca-HCO ₃	A
7 ^c	Spring	08/2002	520	7.6	75.0	8.5	4.6	1.0	18.2	6.8	237	-	10.0	3.7	+1.39	Ca-HCO ₃	GF
8	Spring	05/2002	413	7.8	45.6	17.6	6.0	1.0	8.4	15.1	233	0.3	10.0	6.5	-4.48	Ca-Mg-HCO ₃	KF
		08/2002	423	7.5	61.7	14.7	6.3	1.0	15.4	9.4	237	0.7	10.0	4.5	+0.39	Ca-Mg-HCO ₃	KF
9	Well	05/2002	924	7.5	76.3	52.5	22.0	1.0	66.4	65.7	359	1.1	60.0	33.6	-0.40	Mg-Ca-HCO ₃ -Cl	C
		08/2002	910	7.4	73.5	51.3	16.8	1.0	65.0	48.8	349	0.2	67.0	21.2	+0.37	Mg-Ca-HCO ₃ -Cl	C
10	Well	05/2002	1,231	7.5	79.7	63.3	52.0	2.6	101.0	60.8	413	0.7	41.1	32.8	+2.64	Mg-Ca-Na-HCO ₃ -Cl	C
		08/2002	793	7.4	54.7	47.1	39.7	3.0	78.8	32.8	337	0.6	30.0	1.4	-0.31	Mg-Ca-Na-HCO ₃ -Cl	C
11	Well	05/2002	631	7.5	100.0	5.9	11.0	1.0	17.9	6.3	347	0.3	12.0	6.6	-2.93	Ca-HCO ₃	GF
		08/2002	668	7.2	99.1	6.4	8.9	1.0	34.6	7.4	308	0.4	14.8	5.9	-2.61	Ca-HCO ₃	GF
12	Well	05/2002	1,386	7.8	64.7	57.1	132.0	8.5	184.0	60.5	431	0.5	53.0	41.0	+1.26	Na-Mg-Ca-HCO ₃ -Cl	A
		08/2002	1,512	7.4	67.2	61.6	135.0	9.6	187.0	74.4	426	0.6	53.0	22.0	+2.48	Na-Mg-Ca-HCO ₃ -Cl	A
13 ^c	Well	08/2002	939	8.0	68.2	64.0	18.8	1.0	54.4	61.8	420	0.2	36.0	17.6	-1.06	Mg-Ca-HCO ₃	A
14 ^c	Well	05/2002	1,000	7.5	78.2	41.8	56.0	2.1	53.5	44.4	419	0.8	34.2	30.0	+2.54	Ca-Mg-Na-HCO ₃	A
15	Well	05/2002	700	7.5	70.0	23.1	28.0	1.9	55.5	18.3	347	0.3	40.1	16.2	-6.92	Ca-Mg-HCO ₃ -Cl	A
		08/2002	731	7.7	68.2	26.9	26.0	1.6	80.8	17.6	278	-	42.0	9.6	-2.96	Ca-Mg-HCO ₃ -Cl	A
16	Well	05/2002	997	7.4	54.1	45.4	78.0	6.3	94.3	36.4	377	0.2	43.1	31.8	+1.95	Mg-Na-Ca-HCO ₃ -Cl	A
		08/2002	1,103	7.2	66.9	46.7	66.0	5.5	123.0	39.8	408	0.9	54.7	23.5	-3.96	Mg-Ca-Na-HCO ₃ -Cl	A
17	Well	05/2002	802	7.5	86.3	21.7	28.0	3.9	50.0	90.0	287	0.5	15.6	26.0	-3.93	Ca-Mg-HCO ₃ -SO ₄	A
		08/2002	849	7.2	86.9	21.9	29.2	3.9	72.2	66.4	284	0.9	18.8	18.8	-3.93	Ca-Mg-HCO ₃ -Cl	A
18 ^c	Sea	05/2002	5,8600	8.2	461.0	1,480	1,2600	603	22,560	3,098	452	-	-	-	+0.01	Na-Cl	-

^aElectrical Conductivity ($\mu\text{Siemens cm}^{-1}$)

^bPercent (%) Charge Balance Error = $[\sum \text{cations} - \sum \text{anions}] / [\sum \text{cations} + \sum \text{anions}] \times 100$

^cWater samples are not used in the multivariate statistical analysis

^dThis is the geologic formation from which a spring originates or a well is being fed (A alluvium, C caliche, GF güvenç formation, KF karaisali formation)

as much information as the equivalent of one original variable, it is dropped (StatSoft Inc. 1997). The reader is referred to the work of Davis (1986) for an in-depth account of the theory.

Aqueous geochemical modeling

Inverse modeling calculations were performed using PHREEQC (Parkhurst and Appelo 1999). PHREEQC was also used to calculate aqueous speciation and mineral saturation indices. Inverse modeling in PHREEQC uses the mass-balance approach to calculate all the stoichiometrically available reactions that can produce the observed chemical changes between end-member waters (Plummer and Back 1980). This mass balance technique has been used to quantify reactions controlling water chemistry along flowpaths (Thomas et al. 1989) and quantify mixing of

end-member components in a flow system (Kuells et al. 2000). Minerals used in the inverse geochemical models are limited to those present in the study area. Finally, the mineral reaction mode (dissolution or precipitation) is constrained by the saturation indices for each mineral (Table 2).

Results

Hierarchical cluster analysis

The May 2002 dataset were classified by HCA in 12-dimensional space and presented in a dendrogram (Fig. 4a). Two preliminary groups are selected based on visual examination of the dendrogram each representing a hydrochemical facies. The choice of number of clusters is subjective and choosing the optimal number of groups depends on the researcher since there is no test to

Table 2 Saturation indices (SI) of the water samples (from May and August 2002 sampling campaigns) with respect to various mineral phases

Phases	Water Sample IDs																	
	1	2	3	4	5	6	7	8	9	10	11	12	13	14	15	16	17	18
Amorphous Silica	-0.97	-1.03	-1.03	-0.57	-0.56	-0.76	-	-1.03	-0.25	-0.41	-0.95	-0.30	-	-0.49	-0.42	-0.39	-0.83	-
Calcite	0.49	0.58	0.69	0.32	0.57	0.25	-	0.39	0.41	0.47	0.57	0.68	-	0.49	0.40	0.19	0.38	1.30
Aragonite	0.34	0.43	0.55	0.18	0.42	0.10	-	0.24	0.26	0.33	0.42	0.53	-	0.34	0.25	0.05	0.24	1.16
Dolomite	0.71	1.05	0.85	0.75	1.32	0.56	-	0.64	0.95	1.13	0.19	1.60	-	1.00	0.61	0.60	0.45	3.45
Gypsum	-2.43	-2.61	-2.47	-2.07	-1.99	-2.13	-	-2.55	-1.85	-1.90	-2.66	-2.00	-	-2.00	-2.36	-2.23	-1.62	-0.56
Anhydrite	-2.66	-2.84	-2.70	-2.31	-2.23	-2.37	-	-2.79	-2.09	-2.14	-2.89	-2.24	-	-2.24	-2.60	-2.47	-1.85	-0.77
Halite	-8.13	-8.45	-8.84	-7.51	-8.01	-8.20	-	-8.85	-7.42	-6.87	-8.27	-6.21	-	-7.11	-7.38	-6.72	-7.43	-2.36
August 2002	1	2	3	4	5	6	7	8	9	10	11	12	13	14	15	16	17	18
Amorphous Silica	-0.85	-0.91	-1.03	-0.92	-0.54	-0.67	-1.03	-1.03	-0.20	-0.55	-0.85	-0.30	-0.47	-	-0.40	-0.29	-0.75	-
Calcite	0.13	0.38	0.25	0.07	0.61	0.21	0.41	0.22	0.29	0.16	0.22	0.30	0.91	-	0.50	0.11	0.09	-
Aragonite	-0.02	0.23	0.11	-0.08	0.46	0.07	0.26	0.08	0.15	0.02	0.07	0.15	0.76	-	0.35	-0.04	-0.06	-
Dolomite	-0.05	0.57	0.10	-0.15	1.51	0.50	0.15	0.11	0.72	0.55	-0.47	0.84	2.08	-	0.87	0.35	-0.13	-
Gypsum	-2.54	-2.60	-2.68	-2.57	-2.24	-2.20	-2.70	-2.64	-1.98	-2.26	-2.59	-1.91	-1.95	-	-2.39	-2.12	-1.74	-
Anhydrite	-2.78	-2.84	-2.92	-2.80	-2.47	-2.44	-2.93	-2.88	-2.22	-2.50	-2.82	-2.15	-2.18	-	-2.63	-2.36	-1.98	-
Halite	-8.02	-8.28	-8.64	-8.32	-7.80	-8.09	-8.64	-8.57	-7.54	-7.08	-8.08	-6.20	-7.58	-	-7.25	-6.68	-7.25	-

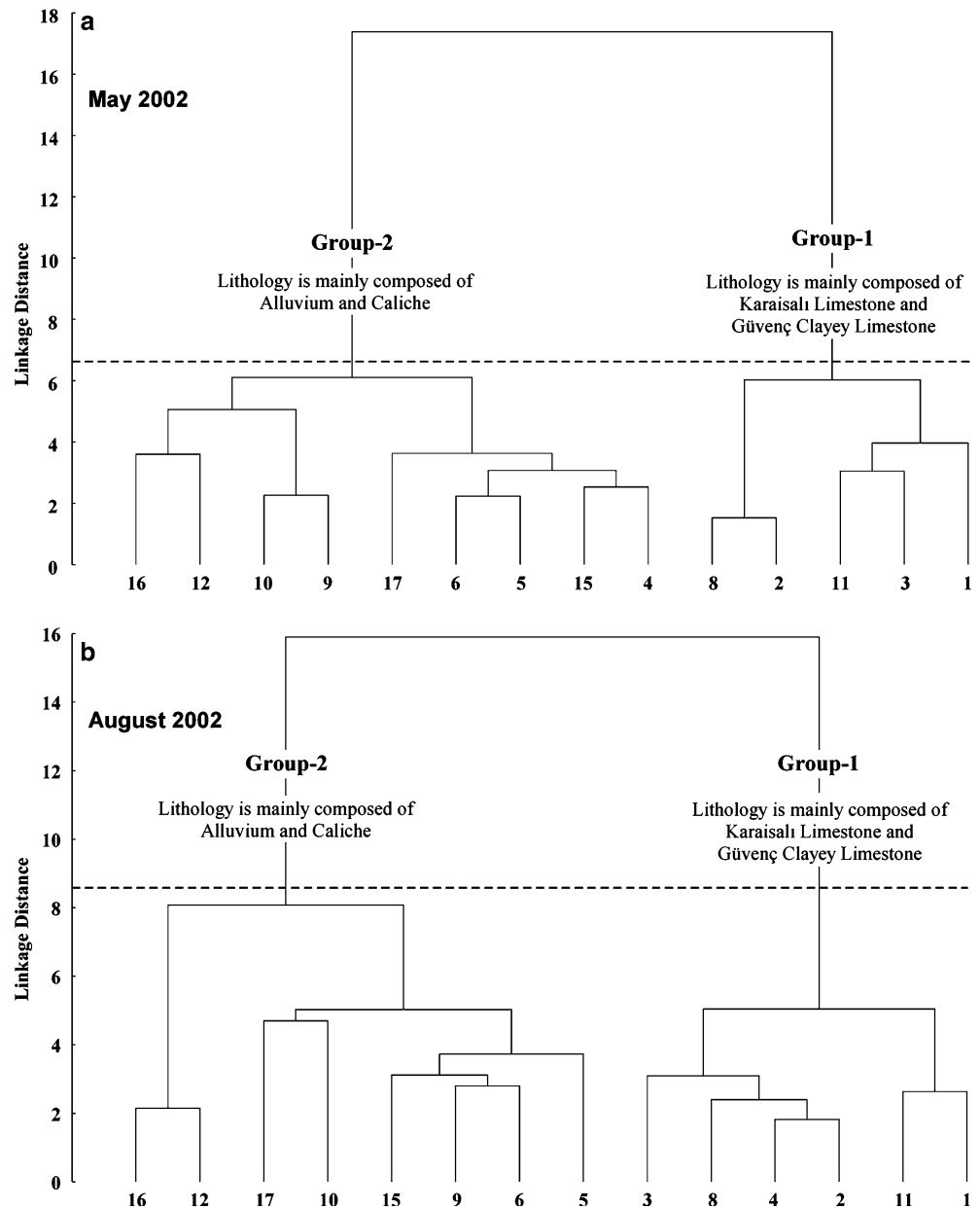
Saturation index (SI) = $\text{Log} \frac{[\text{Ion Activity Product}]}{K_T}$ where K_T = equilibrium constant at temperature T . Phases and thermodynamic data are from PHREEQC and accompanying databases (Parkhurst and Appelo 1999). Saturation indices were calculated by the computer program PHREEQC (Version 2.0) (Parkhurst and Appelo 1999)

determine the optimum number of groups in the dataset (Güler et al. 2002). However, the large linkage distance between groups-1 and -2 (Fig. 4a) suggests that two clusters exist for the May 2002 dataset. Detailed evaluation of the data (comparing Fig. 4a and Table 1) revealed that group-1 samples (for the May dataset) are almost exclusively composed of spring water (except one well water sample; 11). Whereas, group-2 samples are consisted of well water (except one spring water sample; 4), indicating that the spring and well waters maintain distinct chemical signatures. The lithology (i.e., water-rock interaction) seems to be a major component that is affecting the water chemistry in the region. For instance, group-1 samples are mostly found within the limestones (Karaisalı and Güvenç formations); however, group-2 samples are mostly found within the alluvium and to a lesser extent within the caliche (Table 1 and Fig. 4a). It is also worth to note that group-1 samples are mostly found geographically at higher altitudes than group-2 samples, which are mostly located along the coast within the Quaternary basin-fill deposits (Fig. 1).

August 2002 dataset were also classified by HCA in 12-dimensional space and are presented in a dendrogram (Fig. 4b). Two preliminary clusters were chosen for this dataset as well. In the dendrogram, group-1 samples are composed primarily of spring water (except one well water sample; 11) and group-2 samples are exclusively consisted of well water. The only difference between the groupings of the May and August datasets is the sample number 4 (spring water), which is classified as group-1 in August and as group-2 in May (Fig. 4a, b). This difference in the grouping of the sample 4 is due to a large difference in the water chemistry between May and August sampling periods for this locale, in which in August all ion concentrations drop nearly 50% possibly due to mixing with a more diluted water source. However, no reasonable explanation can be given for the source of the diluting component for this karstic spring, since there was virtually no precipitation during August 2002 sampling campaign. Another possibility is that a pollution might have been occurred during May 2002 and concentrations of major ions returned their natural levels in August when this pollution source ceased. This explanation seems logical since the highest irrigation frequency and fertilizer/fungicide applications occur during May–June period.

Overall, both May and August datasets show similar patterns (Fig. 4a, b). Group-1 samples are mostly found within limestone formations and they are mostly composed of spring water samples. Group-1 samples can be classified as Ca-Mg-HCO₃, Mg-Ca-HCO₃, and Ca-HCO₃ water types (Table 1), which suggests the carbonate rocks play an important role in the chemistry of these group of waters. On the other hand, group-2 samples are mostly found in alluvium and they are almost exclusively composed of well water samples.

Fig. 4 Dendrograms of Q-mode HCA showing associations between samples from different parts of the hydrologic system for May (a) and August (b) sampling campaigns. *Dashed line* is “phenon line”, which is chosen by analyst to select number of groups. The numbers in the x-axis represent the same individual sampling locations as in Table 1



Group-2 samples can be classified as various mixed type waters (Table 1) and variations in their chemistries can be explained by natural lithological and geological variations observed in the detrial aquifer materials. As it was mentioned earlier, the basin-fill deposits vary greatly in lithology, grain-size and aquifer properties (both vertically and areally) hence creating observed diverse water chemistries. The overall pattern shows that the water chemistry in the MEB area is mostly affected by aquifer lithology and water–rock interaction is the dominant process creating the natural variability observed in the water chemistries. However, within the MEB aquifer there are several locations where anthro-

pogenic processes dominate the water chemistry (see below for further discussion).

Principal components analysis

Principal components analysis (PCA) was used to reduce the number of variables and identify the variables most important in separating the groups, in effect extracting the factors that control the chemical variability. In this analysis, the axes (principal components) may represent the dominant underlying processes and should help constrain any process-based models of hydrochemical

evolution. In this situation, we anticipate that the chemistry of groundwater is derived from typical water–rock interaction (weathering) as precipitation reacts with aquifer minerals during flow. In addition, there may be contributions from anthropogenic sources that can produce distinct chemical differences compared to natural background. This technique can highlight those outliers or groups of samples that are controlled by such factors from the more pervasive natural background. Detailed analysis showed that three PCs are the most meaningful choice for the system.

For the May 2002 dataset, three significant PCs explain 81.8% of the variance of the original dataset. Most of the variance is contained in the PC1 (59.3%), which is associated with the variables EC, Mg, Na, K, Cl, HCO₃, and SiO₂ (Table 3). PC2 explains 13.0% of the variance and is mainly related to Ca. The variables SO₄, F, and NO₃ contribute most strongly to the third component (PC3) that explains 9.5% of the total variance. PC1 and PC2 contain classical hydrochemical variables originating from weathering processes, whereas the PC3 is related to SO₄, F, and NO₃. High concentrations of nitrate is generally attributed to anthropogenic sources.

For the August 2002 dataset, three PCs explain 82.6% of the variance. Most of the variance is contained in the PC1 (57.3%), which is associated with the variables EC, Mg, Cl, SO₄, HCO₃, SiO₂, and NO₃. PC2 explains 16.5% of the variance and is related to Ca. The variables Na, K, and F contribute most strongly to the third component (PC3), which explains 8.8% of the total variance (Table 3). This pattern is different from the one that was seen in the May 2002 dataset and may indicate a seasonal difference in the processes that affect the water chemistries. It is particularly interesting that in May samples, SO₄ and NO₃ concentrations are abnormally higher than August samples (Table 1) and these two variables (SO₄ and NO₃) strongly contribute to the PC3. As MEB is surrounded by an area rich in citrus orchards, traditional farms and greenhouses, an agricultural source for NO₃ and SO₄ is possible. Use of

fertilizers (a nitrate source) and copper sulfate (CuSO₄) is very widespread practice in the agricultural activities of the area. Copper sulfate is a fungicide used to control bacterial and fungal diseases of fruit, vegetable, and field crops. It is used in combination with lime and water as a protective fungicide, referred to as Bordeaux mixture.

The occurrence of high concentrations of nitrate and sulfate in May samples also coincides with the highest irrigation frequency (during the early periods of plant/vegetable development), which occurs during early summer (May–June). A possible mechanism for these ions in reaching the underlying aquifer can be their mobilization with the irrigation return water. High permeability units (coarse sand-gravel and karstic limestones) within the study area possibly provide the fast pathways for the irrigation return water reaching the underlying aquifer within relatively short time scales (e.g., weeks to months). Interestingly, nitrate and sulfate concentrations drop their normal levels in the groundwater in August, during which irrigation is in its lowest and evapotranspiration in its highest. Therefore, PC3 can be considered as an anthropogenic factor that is only affecting the water chemistry during early summer months (May–June).

Figure 5 shows the projection of the three PC scores (PC1 vs. PC2 vs. PC3) for May (a) and August (b) datasets in a 3D scatter-plot. The distribution of PC scores for both May and August 2002 datasets suggest a continuous variation of the chemical and physical properties of some of the samples. In Fig. 5, for both datasets, groups-1 and -2 samples are well separated in the PC space and completely consistent with the HCA derived groupings. Compact PC distributions for majority of the water samples within groups suggest that all the water samples in their respective groups have similar chemistries hence similar flowpaths or sources. If distribution of the samples in the PC space is broad it may indicate changes in the water chemistry due to processes such as a source of contamination, dilution or abrupt changes in vertical–horizontal connectivity of the

Table 3 PCA loadings for May and August 2002 datasets. Significant loadings are in bold and italic

Variables	May 2002			August 2002		
	PC1	PC2	PC3	PC1	PC2	PC3
pH	-0.501	-0.532	0.013	0.033	-0.858	-0.255
EC	<i>0.863</i>	0.194	0.398	<i>0.828</i>	0.149	0.499
Ca	0.030	<i>0.947</i>	0.068	0.046	<i>0.937</i>	-0.095
Mg	<i>0.651</i>	-0.338	0.559	<i>0.749</i>	-0.490	0.327
Na	<i>0.956</i>	0.041	0.193	0.642	0.033	<i>0.740</i>
K	<i>0.895</i>	-0.155	0.028	0.358	0.085	<i>0.795</i>
Cl	<i>0.883</i>	0.115	0.347	<i>0.736</i>	0.116	0.603
SO ₄	0.577	-0.104	<i>0.663</i>	<i>0.777</i>	-0.133	0.460
HCO ₃	<i>0.794</i>	0.323	0.207	<i>0.792</i>	0.068	0.370
F	0.148	0.211	<i>0.916</i>	0.155	-0.105	<i>0.702</i>
SiO ₂	<i>0.773</i>	0.056	0.502	<i>0.884</i>	-0.130	0.269
NO ₃	0.373	-0.145	<i>0.650</i>	<i>0.812</i>	0.130	-0.176

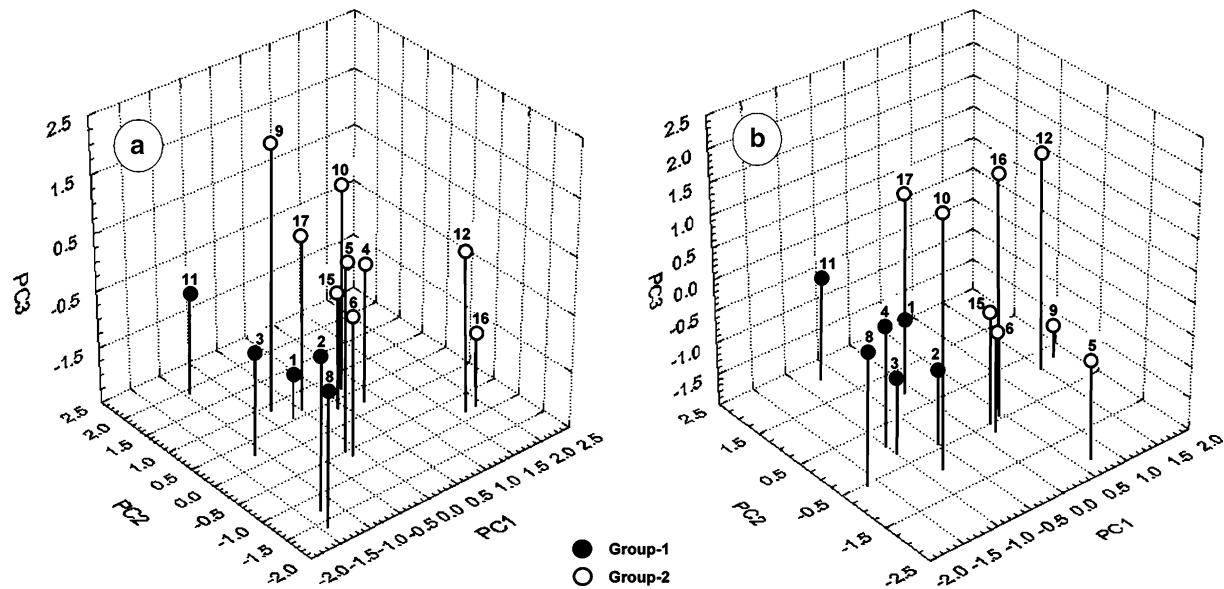


Fig. 5 PCA loading 3D plots (PC1 vs. PC2 vs. PC3) for 14 water samples of May (a) and August (b) sampling campaigns

aquifer. For instance, in both May and August 3D scatter-plots, samples 12 and 16 (both group-2 samples) show differences from their respective group members (Fig. 5a, b). These wells display considerably high Na, K, and Cl concentrations (Table 1). High concentrations of these ions are generally attributed to seawater intrusion. However, considering the location of sample 16 and low concentrations of these ions in samples 13, 14, and 17 render this scenario as unlikely (Fig. 1).

Geochemical modeling

Inverse modeling is often used for interpreting geochemical processes that account for the hydrochemical evolution of groundwater (Plummer et al. 1983). This mass balance approach uses two water analyses represent starting (initial) and ending (final) water compositions along a flowpath to calculate the moles of minerals and gases that must enter or leave solution to account for the differences in composition. We use the information from the lithology, general hydrochemical evolution patterns, and saturation indices (Table 2) to constrain the inverse models. Inverse models for the observed changes between samples 11, 10, and 12 were formulated (starting with 11 and ending with 12). These samples were chosen because they are the only samples in the area that are aligned along the natural groundwater flow direction, which is from north to south. These wells also display high Na, K, and Cl concentrations and it will be tested if their water chemistries could be generated by simple water–rock interaction rather than seawater intrusion.

The chemical composition of minerals in the Taurus Mountains and basin-fill imposes a fundamental constraint on the selection of the mineral phases that will be used in geochemical calculations. The inverse models were formulated so that primary mineral phases including plagioclase, K-feldspar, biotite, hornblende, and olivine are constrained to dissolve until they reach saturation, and calcite, amorphous silica, kaolinite and smectite were set to precipitate once they reached saturation. Halite and gypsum are included as sources of Cl and SO_4 , respectively. Finally, ion exchange is added to the models, which is possibly an important process in the coastal aquifer. We will use the samples 11, 10, and 12 from the August 2002 dataset for the inverse geochemical modeling. Ideally the data for inverse modeling is from a steady-state condition, but in fact few natural hydrologic systems ever reach steady state and this procedure has been widely applied with useful results. The preliminary hydrochemical evolution is based on the behavior of individual components within the context of PCA analysis. The fundamental premise is that TDS increases as water moves from the recharge to the discharge areas. The process of systematic increases in most parameters continues until an upper limit is reached due to mineral equilibrium (e.g. calcite saturation). This conceptual model is supported by the PCA results that showed the majority of variation in the dataset was related to components associated with dissolution of major aquifer minerals (Na, K, Mg, and Ca).

The inverse geochemical modeling using PHREEQC demonstrated that relatively few phases are required to derive water chemistry in the area. In a broad sense, the

reactions responsible for the hydrochemical evolution (along the flowpath from 11 to 10 and 10 to 12) in the area fall into four categories: (1) silicate weathering reactions; (2) dissolution of salts; (3) precipitation of calcite, amorphous silica and kaolinite; (4) ion exchange.

The evolution of waters (from samples 11 to 10; see Fig. 1 for locations) can be explained by the weathering of a relatively small number of primary minerals (total 10) found in the study area. An inverse model describing the evolution can be written as shown below.

Model 1: Ca-HCO₃ water (Sample 11) + Plagioclase + K-feldspar + Halite + Gypsum + Mg from ion exchange + CO₂ gas → Mg-Ca-Na-HCO₃-Cl water (Sample 10) + Kaolinite + Calcite + Amorphous silica + Na loss to ion exchange.

Based on the Model 1, dissolved constituents in the sample 10 water come primarily from weathering reactions of plagioclase and K-feldspar and from dissolution of halite and gypsum. Elevated magnesium concentration in sample 10 water is likely related to the ion exchange (Na replacing Mg in smectitic clays found in the area).

As sample 10 water moves toward Mediterranean Sea, concentrations of major-ions increase, producing sample 12 water (Table 1). The increase in major-ion concentrations of sample 12 water is a result of groundwater interactions with the basin-fill deposits and the same set of minerals used in Model 1 explain the chemistry of the sample 12 water. An inverse model for the processes is:

Model 2: Mg-Ca-Na-HCO₃-Cl water (Sample 10) + Plagioclase + K-feldspar + Halite + Gypsum + Mg from ion exchange + CO₂ gas → Na-Mg-Ca-HCO₃-Cl (Sample 12) + Kaolinite + Calcite + Amorphous silica + Na loss to ion exchange.

The Na:Cl molar ratios of samples 11, 10, and 12 (samples ordered along the flowpath) and the seawater (Na:Cl=0.40, 0.78, 1.11, and 0.86, respectively) suggest that the sodium and chloride contents of these samples is mostly derived from water-rock interaction since Na:Cl molar ratios increase gradually along the flowpath and sample 12 (closest to sea) has a Na:Cl molar ratio that is higher than the seawater.

Discussion

The results of this study showed that quantitative analysis of hydrochemical data using classical multivariate statistical and hydrochemical techniques can help elucidate the hydraulic and geologic factors controlling water chemistry on the regional scale. The integrated statistical/spatial/geochemical analysis showed that some locations have water chemistry due to natural water-rock interactions, while other locations were impacted by an anthropogenic source or sources.

As determined by PCA analysis, anthropogenic factors show seasonality in the area where most contaminated waters related to fertilizer and fungicide applications that occur during early summer season (May–June). This period also coincides with the application of the highest irrigation frequency during the early periods of plant/vegetable development. MEB area is particularly vulnerable to agricultural pollution sources because rapid flow rates (due to coarse sediments and karstic features) produce limited opportunity for natural processes that attenuate anthropogenic pollution. Springs seem to be less prone to anthropogenic pollution as indicated by their relatively low nitrate concentrations during both May and August sampling campaigns (Table 1). This is probably because all the springs in the area are used as a drinking water source (for villages) and protective measures were taken to ensure that no pollution sources exist within the close vicinity of these areas. However, particular caution should be taken for the safety of sample 4 (spring water), which seem to be polluted during May 2002.

On the other hand, wells in the MEB are showed normal background chemistry in August, but in May the water quality had degraded due to anthropogenic impact. Agriculture in this region is dominated by intensive citrus orchards, small crop and vegetable production, with high rates of nitrogen fertilizer and fungicide (copper sulfate) applications. Nitrate pollution of groundwaters in these areas is of particular concern because of the large number of people in cities and rural areas relying on groundwaters for drinking water. However, nitrate concentrations in all wells were below the maximum permissible limit for drinking water (50 mg L⁻¹). Nitrate in most of these wells was likely to have come directly from fertilizer, however other organic sources is also possible, such as sewage and septic overflows.

At locations where groundwater quality in May is not as good as in August, it can be inferred that there is good hydraulic connection between the surface and aquifer. Locations with no significant change in water quality between sample periods have poor vertical hydraulic connection (e.g., sample 11, only well within the Güvenç formation). Based on the distribution of such locations we can see that the scale of heterogeneity is small since adjacent wells such as 10 and 11, where one well shows the pollution effect (23 times increase in NO₃ content), while adjacent well 11 does not. In the area, EC values commonly increase dramatically between the upper slope locations and those on the delta plain over horizontal distances of only 1–3 km. EC values of groundwater from the upper slopes are typically ~700 μS/cm, whereas, groundwater samples from the delta plain have EC values over ~1,500 μS/cm. However, in some regions this increase in EC values is not observed and groundwater from the lower slopes and the delta plain is

relatively fresh (samples 5 and 6). The overall pattern in the MEB area is low EC values in the higher elevations in the north and higher EC values at the lower elevations to the south. This pattern is consistent with the expectation that greater rock–water interactions will increase EC values along topographic flowpaths. Spatial coherence of the statistical clusters is expected in a system where water chemistry is dominated by a few underlying hydrochemical processes. Further, any clusters defined by Q-mode analysis can reflect the spatial distribution of lithological or hydrochemical conditions that represent the underlying processes.

In summary, the inverse geochemical modeling demonstrated that relatively few phases are required to

derive observed changes in water chemistry and to account for the hydrochemical evolution of groundwater in the area. However, the modifying processes in the coastal zone of this aquifer are complex and do not show a homogeneous pattern in space. Silty-clay intercalations occur in the coastal sector and these favor ionic exchange, in addition, they are also prone to anthropogenic pollution and these two factors make it difficult to interpret all the processes occurring.

Acknowledgments The authors are pleased to acknowledge the cooperation and support of the General Directorate of Mineral Research and Exploration (MTA), Ankara, Turkey. The authors also thank MTA staff for their support with field operations and assistance with sample collection.

References

- Davis JC (1986) *Statistics and data analysis in geology*. 2nd edn. Wiley Inc, NY
- Demirel Z (2004) The history and evaluation of saltwater intrusion into a coastal aquifer in Mersin, Turkey. *J Environ Man* 70:275–282
- Güler C, Thyne G, McCray JE, Turner AK (2002) Evaluation of graphical and multivariate statistical methods for classification of water chemistry data. *Hydrogeol J* 10:455–474
- Helena B, Pardo R, Vega M, Barrado E, Fernandez JM, Fernandez L (2000) Temporal evolution of ground water composition in an alluvial aquifer (Pisuerga River, Spain) by principal component analysis. *Water Res* 34:807–816
- Hidalgo MC, Cruz-Sanjulian J (2001) Ground water composition, hydrochemical evolution and mass transfer in a regional detrital aquifer (Baza basin, southern Spain). *Appl Geochem* 16:745–758
- Judd AG (1980) The use of cluster analysis in the derivation of geotechnical classifications. *Bull Assoc Eng Geol* 17:193–211
- Kaiser HF (1960) The application of electronic computers to factor analysis. *Educ Psychol Meas* 20:141–151
- Kuells C, Adar EM, Udluft P (2000) Resolving patterns of ground water flow by inverse hydrochemical modeling in a semiarid Kalahari basin. *Tracers Model Hydrogeol* 262:447–451
- Meng SX, Maynard JB (2001) Use of statistical analysis to formulate conceptual models of geochemical behavior: water chemical data from the Botucatu aquifer in São Paulo state, Brazil. *J Hydrol* 250:78–97
- Ochsenkühn KM, Kontoyannakos J, Ochsenkühn PM (1997) A new approach to a hydrochemical study of ground water flow. *J Hydrol* 194:64–75
- Parkhurst DL, Appelo CAJ (1999) *User's guide to PHREEQC (Version 2)–A computer program for speciation, batch-reaction, one-dimensional transport, and inverse geochemical calculations*. USGS Water Res Invest Rep 99–4259
- Plummer LN, Back WW (1980) The mass balance approach-application to interpreting the chemical evolution of hydrological systems. *Am J Sci* 280:130–142
- Plummer LN, Parkhurst DL, Thorstenson DC (1983) Development of reaction models for ground-water systems. *Geochim Cosmochim Acta* 47:665–686
- Pulido-Leboeuf P (2004) Seawater intrusion and associated processes in a small coastal complex aquifer (Castell de Ferro, Spain). *Appl Geochem* 19:1517–1527
- Qian G, Gabor G, Gupta RP (1994) Principal components selection by the criterion of the minimum mean difference of complexity. *J Multivariate Anal* 49:55–75
- Reeve AS, Siegel DI, Glaser PH (1996) Geochemical controls on peatland pore water from the Hudson Bay Lowland; a multivariate statistical approach. *J Hydrol* 181:285–304
- Senol M (1998) The geological investigation of Mersin region. General Directorate of Mineral Research and Exploration of Turkey, Ankara (in Turkish)
- StatSoft Inc (1997) *Electronic Statistics Textbook*, Tulsa, OK <http://www.statsoft.com/textbook/stathome.html>
- StatSoft Inc (2000) *STATISTICA for Windows [Computer program manual]*. Tulsa, OK
- Swanson SK, Bahr JM, Schwar MT, Potter KW (2001) Two-way cluster analysis of geochemical data to constrain spring source waters. *Chem Geol* 179:73–91
- Thomas JM, Welch AH, Preissler AM (1989) Geochemical evolution of ground water in Smith Creek Valley—a hydrologically closed basin in central Nevada, USA. *Appl Geochem* 4:493–510
- Ward JH (1963) Hierarchical grouping to optimize an objective function. *J Am Stat Assoc* 69:236–244
- Yaman S (1991) Mersin ofiyolitinin jeolojisi ve metalojenisi. Ahmet Acar Jeoloji Sempozyumu Bildirileri. Çukurova Üniversitesi Mühendislik-Mimarlık Fakültesi: 255–268 (in Turkish)